# Structure of Zn–Se–Te system with submonolayer insertion of ZnTe grown by migration enhanced epitaxy

Y. Gong[a] and Hanfei F. Yan
*Department of Applied Physics and Applied Mathematics, Columbia University, New York, New York 10027*

I. L. Kuskovsky
*Queens College of CUNY, Flushing, New York 11367*

Y. Gu, I. C. Noyan, and G. F. Neumark
*Department of Applied Physics and Applied Mathematics, Columbia University, New York, New York 10027*

M. C. Tamargo
*Department of Chemistry, City College of CUNY, New York, New York 10031*

(Received 17 June 2005; accepted 7 February 2006; published online 31 March 2006)

We here report results of high resolution x-ray diffraction, x-ray reflectivity (XRR), as well as optical absorption and reflection measurements on ZnSe samples grown by molecular beam epitaxy, with insertion of planar ($\delta$-) regions of both N as an acceptor dopant and Te as a "co-dopant" to facilitate a *p*-type doping. We note that to enhance the surface diffusion of Te, migration enhanced epitaxy was adopted in the growth of the "$\delta$-layers;" i.e., Te is deposited in the absence of Zn flux. Structural parameters were extracted by simulating the experimental x-ray diffraction curves using a dynamical model. The results show that only the "$\delta$-layers" (with submonolayer thickness) are rich in ZnTe, while the nominally undoped "spacers" have only a low Te concentration. Moreover, the morphology of the surface and interfaces are studied by XRR. Furthermore, the optical absorption and reflection results show that our samples largely preserve the optical properties of the host material (ZnSe). We note that our results, in particular those on the Te concentration, explain the observed good *p*-type doping of such samples. © *2006 American Institute of Physics*.
[DOI: 10.1063/1.2184434]

## I. INTRODUCTION

It is well known that it has been difficult to obtain a good *p*-type ZnSe. The use of Zn–Se–Te multilayer systems for improving *p*-type doping has been suggested (e.g., Ref. 1 and references therein) since ZnTe is easily doped *p*-type.[2,3] We have developed a planar ($\delta$-) (Ref. 1) doping technique, involving the use of N as an acceptor dopant together with Te as a "co-dopant" to facilitate the *p*-type doping in ZnSe. A net acceptor concentration as high as $6\times10^{18}$ cm$^{-3}$ (Ref. 1) was achieved in samples with regions of three contiguous "$\delta$-layers" of [N+Te], where these regions will hereupon be referred to simply as "$\delta$-layers," and such samples will be referred to as $\delta^3$-ZnSe:(Te,N). In practice, the deposition is carried out by molecular beam epitaxy (MBE), with the [N+Te] "$\delta$-layers" deposited on top of nominally pure undoped ZnSe layers ("spacers") and where the "$\delta$-layers" are deposited on Zn terminated surfaces. We note that during the growth of the "$\delta$-layers," Te is deposited in the absence of Zn flux, i.e., a growth technique called migration enhanced epitaxy (MEE).[4] Since there is no immediate bond formation, a fast Te diffusion can take place. Moreover, the deposition times of the "$\delta$-layers" (usually 5*s*) resulted in depositions of submonolayer amounts. Details of our growth procedure have been described elsewhere.[1] We also note that a good *p*-type doping in $ZnSe_{1-x}Te_x$ bulk alloys is achieved only for $x\geqslant15\%$.[5] Of high interest now is the mechanism which provides such good doping in the $\delta^3$-ZnSe:(Te,N) samples. To help determine this mechanism, we here study this system via high resolution x-ray diffraction (HRXRD), x-ray reflectivity (XRR), as well as optical absorption and reflection measurements.

High resolution x-ray diffraction is a very effective technique to investigate structural properties of multilayer systems (including a multilayer heterostructure containing quantum dots) due to its high sensitivity to spatial long-range periodicity and strain distribution in examined materials as well as to nondestructive characteristics.[6–9] We note that with a large beam size (of the order of square milimeters), x-ray diffraction experiments investigate overall properties of epitaxial films. By analyzing HRXRD results,[6,9] the following parameters can be extracted by simulating x-ray diffraction curves: (i) periodicity, (ii) period dispersion [we hereupon assume a Gaussian distribution of the period, $T$, with a standard deviation of $\sigma(T)$], (iii) individual layer thickness, and (iv) alloy composition. X-ray reflectivity has been widely used to characterize the morphology of surfaces and interfaces, as reflectivity, a function of incidence angle, depends on the layer thickness, interface roughness, as well as composition profile.[10–12] Low temperature optical absorption and reflection measurements are widely used to investigate the optical properties of materials, including epitaxial layers in

[a]Electronic mail: yg2002@columbia.edu

 © 2006 American Institute of Physics

Downloaded 23 May 2006 to 149.4.205.22. Redistribution subject to AIP license or copyright, see http://jap.aip.org/jap/copyright.jsp

particular.[13–19] With proper analysis of the optical absorption (OA) and reflection spectra, the optical properties, specifically the band gap energy, can be determined. Once the band gap is known, the alloy composition can be calculated using the dependence of the band gap on the alloy composition.

Here, we report results of triple axis HRXRD, XRR, as well as optical absorption and reflection measurements of Zn–Se–Te multilayers with submonolayer insertion of ZnTe [denoted as $\delta^3$-ZnSe:(Te,N)] grown on (001) GaAs substrates. ZnSe spacers were grown by MBE, and submonolayer ZnTe insertions ("$\delta$-layers") were grown by MEE.[1] Structural parameters were extracted by simulating HRXRD experimental results using dynamical diffraction theory from Takagi[20] and Taupin.[21] Our HRXRD results have shown that only the "$\delta$-layers" are rich in ZnTe, while the spacers have a very low Te concentration, less than 5%. Furthermore, in each period, the average thickness of the "$\delta$-layers" is less than 1 monolayer (ML) (1 ML=half a unit cell), which is consistent with our previous results.[22] The root-mean-squared (rms) roughness and layer thickness of epitaxial films are extracted by analyzing XRR curves. Results obtained from HRXRD and XRR agree well with each other. Results of optical measurements show that the epitaxial layers of our samples largely preserve the optical properties of the host materials (ZnSe).

## II. EXPERIMENT

We studied two samples: sample A consisting of 200 periods of spacers (10 ML)/$\delta$-layers (nominal thickness less than 1 ML) with a 10 nm thick ZnSe buffer layer and sample B consisting of 244 periods of spacers (9 ML)/$\delta$-layers (nominal thickness less than 1 ML) without a buffer layer.

X-ray measurements were carried out at Beamline X20A at the National Synchrotron Light Source (NSLS) at Brookhaven National Laboratory (BNL). All measurements were made using monochromatic synchrotron radiation at 8 keV ($\lambda$=1.540 56 Å), with a double-crystal Ge (111) monochromator. For x-ray reflectivity measurements, the incident beam size was set to be approximately $0.2\times1$ mm$^2$ by a slit $S_1$, and to define the angular resolution, a slit $S_2$ was put in front of a detector. The specular reflectivity was recorded when varying the incidence angle from below to above the critical angle. For high resolution x-ray diffraction measurements, the incident beam size was set to about $1\times1$ mm$^2$ by a slit $S_1$, and the angular resolution was defined by putting a Si (111) analyzer in front of the detector. Both symmetric (004) and asymmetric (224) reflections in the $\omega$-$2\theta$ mode were measured.

Low temperature ($T$=9 K) optical absorption and reflection measurements were carried out using a closed cycle refrigerator system. A 300 W xenon lamp (continuous wave) coupled to an optical fiber was used as the excitation source. The transmitted light was dispersed through a 3/4 m monochromator and was detected by a thermoelectrically cooled GaAs photomultiplier tube connected to a photon counter.

To prepare the samples for optical absorption measurements, the GaAs substrates were removed by mechanical polishing, followed by selective chemical etching, using a mixture of NaOH (9 ml, 1$M$) and $H_2O_2$ (6 ml, 30%). The remaining $\delta^3$-doped ZnSe:(Te, N) epitaxial layers were kept on a sapphire window, which was mounted on the cold stage of a closed cycle refrigerating system. In order to measure absorbance, $d_s\alpha(h\upsilon)$ (here $d_s$ is the sample thickness and $\alpha(h\upsilon)$ is the absorption coefficient), we first recorded the light intensity $I_0(h\upsilon)$ transmitted through the sapphire window without the film. Then, we recorded the light intensity $I(h\upsilon)$ transmitted with the film on the sapphire window. The absorbance is determined by the well-known formula

$$d_s\alpha(h\upsilon) = -\ln\left[\frac{I(h\upsilon)}{I_0(h\upsilon)}\right]. \quad (1)$$

Low temperature optical reflection measurements were carried out in normal incidence geometry (for a detailed description of this technique, see Ref. 23).

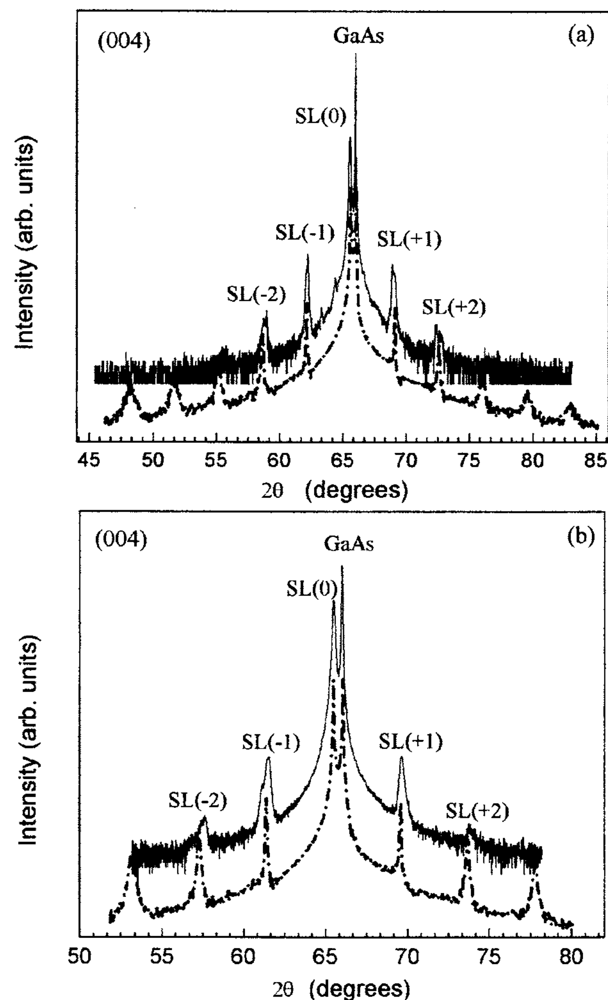


FIG. 1. The (004) $\omega$-$2\theta$ scan curves of samples (a) A and (b) B, both experimental (solid line) and simulated (dotted line). The curves are plotted in log scale and shifted vertically for clarity.

## III. RESULTS AND DISCUSSION

### A. Determination of Te compositions and layer thickness from HRXRD measurements

Figures 1(a) and 1(b) show the symmetric (004) $\omega$-$2\theta$ scans of samples A and B, respectively. The x-ray diffraction

Downloaded 23 May 2006 to 149.4.205.22. Redistribution subject to AIP license or copyright, see http://jap.aip.org/jap/copyright.jsp

TABLE I. Average structural properties of epitaxial films.

| Sample | $\langle c \rangle$ (Å) | $\langle a \rangle$ (Å) | $x_{average}$ | $T$ (Å) |
|---|---|---|---|---|
| A | 5.687 | 5.662 | 2% | 31 |
| B | 5.693 | 5.671 | 4% | 26 |

curves of both samples show similar features. The sharp peak with the highest intensity, located at ~66.006°, is from the GaAs substrate. On both sides of the GaAs peak, superlattice (SL) satellites up to second orders are visible, and all observed SL satellites are distributed with nearly equal angular distances. Thus, the overall periodicity along the growth direction is preserved by introducing the submonolayer $ZnTe_xSe_{1-x}$ ("$\delta$-layers"). Compared with the SL(0), higher order satellites are broadened, which indicates a period dispersion (i.e., fluctuation of periodicity) in our samples.[6,9]

### 1. Estimation of initial fitting parameters

In order to extract the structural parameters of our samples, the measured $\omega$-$2\theta$ scans were simulated.[20,21] The initial parameters of the simulation are obtained as follows.

*a. Average alloy composition.* The average lattice parameter along the growth direction, $\langle c \rangle$, can be calculated directly from the SL(0) peak of the (004) diffraction curve using Bragg's law. Next, we are going to calculate the average in-plane lattice parameter $\langle a \rangle$ based on the results of the asymmetric (224) reflection of our samples (not shown here). We assume that the stresses in the epitaxial layer are equal biaxial in the plane of the film (i.e., $a=b$), i.e., the unit cell is deformed from cubic to tetragonal. For a tetragonal unit cell the interplane spacing $d_{224}$ is a function of latice parameters $a$ and $c$. With known $\langle c \rangle$ and $d_{224}$ [calculated from the peak position of a zero-order satellite on the (224) diffraction], we can obtain $\langle a \rangle$.

Assuming Vegard's law is valid, the average Te composition of the epitaxial layer, $x_{average}$, is given by[24]

$$x_{average} = \frac{[(E\langle a \rangle + \langle c \rangle)/(1+E)] - a_{ZnSe}}{a_{ZnTe} - a_{ZnSe}}, \tag{2}$$

where

$$E = \frac{2\nu}{1-\nu} \tag{3}$$

is the elastic correction factor and $\nu$ is Poisson's ratio. Resultant values of $\langle a \rangle$, $\langle c \rangle$, and $x_{average}$ are listed in Table I.

*b. Periodicity.* The period $T$ is estimated using the angular separation of satellites.[6,9] Since on the (004) diffraction curves of both samples, satellites up to second order are visible, $T$ is calculated by measuring any two satellites and averaging all obtained values (see Table I).

*c. Initial fitting parameters.* Table II lists all structural parameters involved in our simulating process. From the growth procedure, we know that each period contains 10 ML spacers and 9 ML spacers for samples A and B, respectively, and thus, we can determine, assuming a well-controlled growth, $t_1$ of both samples as $10 \times (\langle c \rangle/2)$ and $9 \times (\langle c \rangle/2)$.

TABLE II. Parameters used in simulation.

| | |
|---|---|
| $T$ | Period of multilayers |
| $t_1$ | Thickness of the spacers |
| $t_2$ | Thickness of the "$\delta$-layers" |
| $x_1$ | Te concentration in the spacers |
| $x_2$ | Te concentration in the "$\delta$-layers" |
| $\sigma(T)$ | Period dispersion, defined as the standard deviation of period distribution |

The initial parameters of $t_2$ can be obtained by subtracting $t_1$ from $T$. Since the thickness of the spacers, $t_1$, is much larger than that of the "$\delta$-layers," $t_2$, the average structural properties of the epitaxial layer is dominated by the spacers. Thus, we use $x_{average}$ as our initial fitting parameter for the Te composition in the spacers, $x_1$. Regarding the Te concentration in "$\delta$-layers," we only know from the growth condition that $x_2 \gg x_1$.

### 2. Simulation

For each of our samples, the substrate is a very thick GaAs single crystal, and the epitaxial film has an overall thickness at least ~0.6 $\mu$m, which is close to the extinction depth. Therefore, a dynamical model is preferred for an appropriate simulation. The simulated diffraction intensity is obtained as $|X(0)|^2$, where $X_j \equiv X(z_j)$ is the diffraction coefficient[26] at a given depth $z_j$ below the surface of the film. $X_j$ can be calculated using a recurrence relation

$$X_j = \frac{wX_{j+1} - i(2C\chi_h + uX_{j+1})\tan[\Phi(z_{j+1}-z_j)/2]}{w + i(2gC\chi_{\bar{h}}X_j + u)\tan[\Phi(z_{j+1}-z_j)/2]}, \tag{4}$$

which is a solution of the one-dimensional differential equation given by Halliwell *et al.*[25] Here, $C$ is the polarization factor, which is equal to 1 for a $\sigma$ polarization and $\cos 2\theta$ for a $\pi$ polarization; $\chi_0$, $\chi_{\bar{h}}$, and $\chi_h$ are the Fourier coefficients of the dielectric susceptibility.[27] The other parameters are defined as $\Phi = \pi K w / \cos \gamma_B$, $g = \cos \gamma_B / \cos \beta_B$, $u = (1+g)\chi_0 + 2\eta \sin \theta_B$, $w = \sqrt{u^2 - 4C^2 g \chi_h \chi_{\bar{h}}}$, where $K$ is the wave number of the incident x-ray wave in vacuum, $\eta$ is the deviation angle from the exact Bragg angle $\theta_B$, and $\beta$ and $\gamma$ are angles of the incident beam and the diffracted beam to the surface normal $\mathbf{n}$, respectively.

For our specific system, we assume that the substrate is a perfect single crystal with an infinite thickness; therefore the diffraction coefficient at the interface of the substrate and the epitaxial film can be simply described by

$$X(z=L) = \frac{-u-w}{2gC\chi_{\bar{h}}}, \quad \text{Im}(w) > 0, \tag{5}$$

where $L$ is the total thickness of the thin film. Since $X(L)$ represents the reflection from the substrate, to calculate $X(L)$ the GaAs structural parameters should be used. The diffraction coefficient at the surface, $X(0)$, can be calculated using recurrence relation (4) if the structural parameters for each sublayer in the thin film are known. Then, the simulated diffraction intensity curve is generated as $|X(0)|^2$. During the simulation, we kept $x_1$ and $t_1+t_2$ as close as possible to the

Downloaded 23 May 2006 to 149.4.205.22. Redistribution subject to AIP license or copyright, see http://jap.aip.org/jap/copyright.jsp

TABLE III. Structural parameters extracted by simulating HRXRD data.

| Sample | $t_1$ (Å) | $t_2$ (Å) | $x_1$ | $x_2$ | $T$ (Å) | $\delta(T)$ (Å) |
|---|---|---|---|---|---|---|
| A | 29.40 | 0.73 | 2.2% | 40±15% | 30.13 | 1 |
| B | 24.80 | 0.77 | 4% | 50±15% | 25.57 | 0.8 |

estimated initial parameters listed in Table I, and varied $x_2$ to give the best agreement with the experimental curves.

According to our simulation, intensities of high order SL satellites depend on the Te concentration in the "$\delta$-layers," i.e., the value of $x_2$. If $x_2$ is close to $x_1$, high order SL satellites will become very weak. This is expected because when $x_2$ is equal to $x_1$, the difference between the spacer and the "$\delta$-layers" disappears, and the superlattice structure in the film does not exist. We will not see any SL peak, except for the SL(0) peak. The measured diffraction curve exhibits quite strong high order SL peaks, which indicates the "$\delta$-layers" must have a much higher Te composition than that in spacers. The Te is mainly "locked" in the "$\delta$-layers." The existence of Te-rich "$\delta$-layers" is the main reason for the increase in the net acceptor concentration by more than one order of magnitude despite the fact that only submonolayer quantities of Te are deposited.

As mentioned earlier, the higher order satellites are broadened compared with the SL(0) satellite. It has been suggested[9] that the period difference along the growth direction will contribute to this broadening. Thus, we introduced a Gaussian period dispersion in our simulation with a standard deviation of ~3%. The best fitting curves are shown in Figs. 1(a) and 1(b) as the dotted lines. The corresponding layer thicknesses as well as Te concentrations are listed in Table III.

## B. X-ray reflectivity

We further performed x-ray reflectivity in order to obtain information on the roughness of the interfaces between the spacers and "$\delta$-layers." The rms roughness, chemical profile, and thickness of spacers and "$\delta$-layers" are extracted by comparing the experimental results and computer simulations.[28] We note that to reduce the fitting parameters, we fix the chemical compositions of spacers and "$\delta$-layers" to the values obtained from HRXRD and vary the rms and layer thickness. We found that the thickness of spacers and "$\delta$-layers" agree well with that from HRXRD, and the rms of interfaces are 11.4±1.5 Å and 4.3±1.5 Å, respectively. We note that the rms roughness is much larger than the thickness of "$\delta$-layers." The plausible explanation is that the growth of "$\delta$-layers" forms three-dimensional islands instead of two-dimensional uniform layers. We note that *in situ* reflection high energy electron diffraction[22] (RHEED) shows a three-dimensional (3D) growth mode. Moreover, it has been shown that quantum dots are formed in samples grown under similar conditions without the dopant N.[29,30]

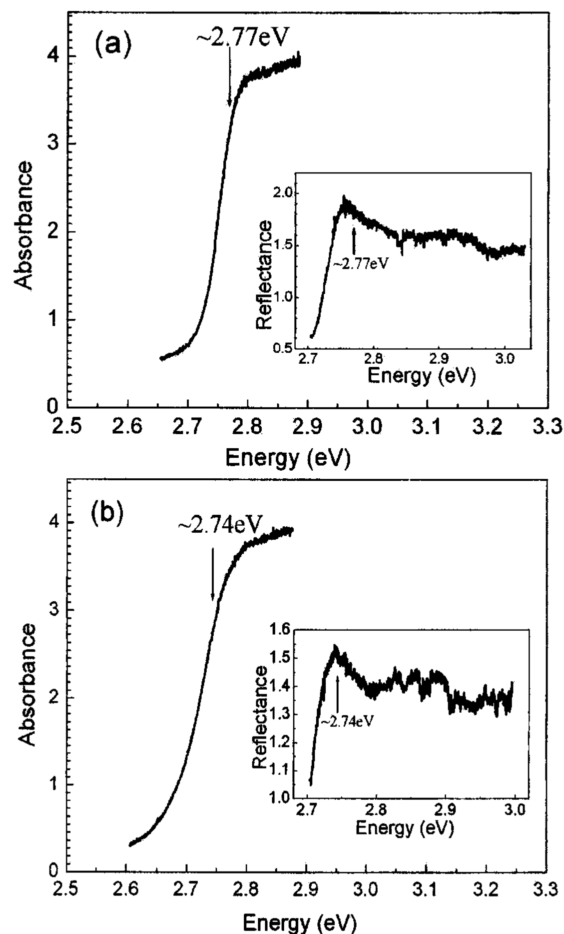


FIG. 2. Low temperature ($T$=9 K) absorption spectra of samples (a) A and (b) B. Insets of (a) and (b) show low temperature ($T$=9 K) reflection spectra of samples A and B, respectively.

## C. Determination of optical band gap and Te composition from optical measurements

Figures 2(a) and 2(b) show low temperature ($T$=9 K) OA spectra of samples A and B, respectively. The insets are the corresponding reflection spectra. Reflectance show an asymmetric maximum value, and the minimum is flattened due to the presence of Te.[31] The absorption spectra have two noteworthy features. The first is that the band edge estimated from the absorption and reflection spectra is at about 2.77 and 2.74 eV, corresponding to ~3% and ~5% Te (e.g., Ref. 32), for samples A and B, respectively. Significantly, the band edges are very close to the ZnSe values. In this connection we would also like to emphasize that the x-ray work has shown that the Te concentrations in the "$\delta$-layers" are about 40%–50% (also see Table III) and that bulk $ZnSe_{1-x}Te_x$ alloys in that concentration range have reflectivity[31] or absorption edges[33] fairly close to the ZnTe values. It is thus apparent that the "$\delta$-layers," despite their overriding effect on the electrical (doping) properties, have at most a very minimal effect on the optical properties. The second interesting feature in the absorption spectra is that the tails in the absorption curves are relatively large. It has been shown[32,34,35] that Te forms various complexes in $ZnSe_{1-x}Te_x$ alloys for ($x \leqslant 2\%$), including $Te_2$ and $Te_{n\geqslant 3}$ complexes; we thus attribute the tails to such complexes.

Downloaded 23 May 2006 to 149.4.205.22. Redistribution subject to AIP license or copyright, see http://jap.aip.org/jap/copyright.jsp

## IV. SUMMARY

High resolution x-ray diffraction, x-ray reflectivity, and optical absorption as well as reflection measurements have been used to study two $\delta^3$-ZnSe:(Te,N) samples grown by MBE (with MEE used in the "$\delta$-layers") on the (001) GaAs substrate. Both samples have similar features for the (004) and (224) diffraction patterns. Thicknesses and alloy compositions of both the "$\delta$-layers" and the spacers have been determined by simulating HRXRD (004) diffraction curves using the dynamical diffraction theory (see Table III). We found that only the "$\delta$-layers," with a thickness ~0.25 ML, are ZnTe rich, while the spacers have low Te concentrations. Moreover, the morphology of the surface and interfaces is investigated by XRR. Furthermore, the optical absorption and reflection results show that our samples largely preserve the optical properties of the host material (ZnSe).

## ACKNOWLEDGMENTS

Part of this work was carried out at the National Synchtron Light Source, Brookhaven National Laboratory, which is supported by the Division of Materials Sciences and Division of Chemical Sciences, U.S. Department of Energy under Contract Nos. DE-AC02-98CH10886 and DE-FG02-05ER46219.


[1]W. Lin, S. P. Guo, M. C. Tamargo, I. L. Kuskovsky, C. Tian, and G. F. Neumark, Appl. Phys. Lett. **76**, 2205 (2000).

[2]C. M. Rouleau, D. H. Lowndes, G. W. McCamy, J. D. Budai, D. B. Poker, D. B. Geohegan, A. A. Puretzky, and S. Zhu, Appl. Phys. Lett. **67**, 2545 (1995).

[3]T. Baron, K. Saxminadayar, and N. Magnea, J. Appl. Phys. **83**, 1354 (1998).

[4]Migration enhanced epitaxy is a variant of conventional MBE, and it occurs when the growing surface is alternatively exposed to group II and group VI elements or to group III and group V elements. For a review, see, e.g., Y. Horikoshi, Semicond. Sci. Technol. **8**, 1032 (1993).

[5]W. Lin, B. S. Yang, S. P. Guo, A. Elmoumni, F. Fernandez, and M. C. Tamargo, Appl. Phys. Lett. **75**, 2608 (1999).

[6]D. Keith Bowen and B. K. Tanner, *High Resolution X-ray Diffractometry and Topography* (Taylor & Francis, London, 1998), Chap. 6.

[7]N. Faleev, K. Pavlov, M. Tabuchi, and Y. Takeda, Jpn. J. Appl. Phys., Part 1 **38**, 818 (1999).

[8]M. Korn, M. Li,S. Tiong-Palisoc, M. Rauch, and W. Faschinger, Phys. Rev. B **59**, 10670 (1999).

[9]P. F. Fewster, *X-ray Scattering from Semiconductors* (Imperial College Press, London, 2003), Chap. 4.

[10]B. Jenichen, S. A. Stepanov, B. Brar, and H. Kroemer, J. Appl. Phys. **79**, 120 (1996).

[11]S. N. Yakunin, E. M. Pashaev, A. A. Zaitsev, A. G. Sutyrin, and V. G. Mokerov, Proc. SPIE **5401**, 573 (2004).

[12]S. Kim, G. Kioseoglou, S. Huang, Y. H. Kao, Y. L. Soo, X. Zhu, and K. L. Wang, J. Appl. Phys. **98**, 074309 (2005).

[13]J. I. Pankove, *Optical Process in Semiconductors* (Dover, Toronto, 1971), Chaps. 2–3.

[14]N. R. Goni, A. Cantareo, K. Syassen, and M. Cardona, Phys. Rev. B **41**, 3641 (1990).

[15]S. A. Clark, P. Roura, J. Bosch, A. Perez-Rodriguez, J. R. Morane, D. I. Westwood, and R. H. Williams, J. Appl. Phys. **77**, 3393 (1994).

[16]P. Y. Yu and M. Cardona, *Fundamentals of Semiconductors* (Springer-Verlag, New York, 1996), Chap. 6.

[17]R. Passler *et al.*, J. Appl. Phys. **86**, 4403 (1999).

[18]J. Wu *et al.*, Phys. Rev. B **68**, 033206 (2003).

[19]G. Bentoumi, V. Timoshevskii, N. Madini, M. Coe, R. Leonelli, J.-N. Beaudry, P. Desjardins, and R. A. Masut, Phys. Rev. B **70**, 035315 (2004).

[20]S. Takagi, Acta Crystallogr. **15**, 1311 (1962).

[21]D. Taupin, Bull. Soc. Fr. Mineral. Cristallogr. **87**, 469 (1964).

[22]Our previous results (unpublished) of the *in situ* reflection high energy electron diffraction (RHEED) and *ex situ* transmission electron microscopy observations have shown that no full monolayer of "$\delta$-layers" is formed.

[23]P. Y. Yu and M. Cardona, *Fundamentals of Semiconductors* (Springer-Verlag, New York, 1996), Chap. 24.

[24]J. L. Jordan-Sweet, P. M. Mooney, M. A. Lutz, R. M. Feenstra, J. O. Chu, and F. K. LeGoues, J. Appl. Phys. **80**, 89 (1996).

[25]M. A. G. Halliwell, M. H. Lyons, and M. J. Hill, J. Cryst. Growth **68**, 523 (1984).

[26]At a given depth $z_j$, for an infinitely thin layer $dz$, $X_j$ is the ratio of the diffracted wave amplitude $D_h(z_i)$ to the incident wave amplitude $D_0(z_i)$.

[27]The imaginary component of $\chi_0$ is negative due to the wave form $\exp(-i2\pi\mathbf{k}\cdot\mathbf{r})$ we choose.

[28]A commercial software BEDE REFs was used to simulate XRR data.

[29]Y. Gu, I. L. Kuskovsky, M. van der Voort, G. F. Neumark, X. Zhou, M. Muňoz, and M. C. Tamargo, Phys. Status Solidi B **241**, 515 (2004).

[30]Y. Gu, I. L. Kuskovsky, M. van der Voort, G. F. Neumark, X. Zhou, and M. C. Tamargo, Phys. Rev. B **71**, 045340 (2005).

[31]A. Yu. Naumov, S. A. Permogorov, A. N. Reznitskiĭ, V. Ya. Zhulaĭ, V. A. Novozhilov, and G. T. Petrovskiĭ, Sov. Phys. Solid State **29**, 215 (1987).

[32]A. Yu. Naumov, S. A. Permogorov, T. B. Popova, A. N. Reznitskiĭ, V. A. Novozhilov, and N. N. Spendiarov, Sov. Phys. Semicond. **21**, 213 (1987).

[33]A. K. Ghosh, K. K. Som, S. Chatterjee, and B. K. Chaudhuri, Phys. Rev. B **51**, 4842 (1995).

[34]I. V. Akimova, A. M. Akhekyan, V. I. Kozlovskiĭ, Yu. V. Korostelin, and P. V. Shapkin, Sov. Phys. Solid State **27**, 1041 (1985).

[35]I. L. Kuskovsky, C. Tian, G. F. Neumark, J. E. Spanier, I. P. Herman, W.-C. Lin, S. P. Guo, and M. C. Tamargo, Phys. Rev. B **63**, 155205 (2001).


**Downloaded 23 May 2006 to 149.4.205.22. Redistribution subject to AIP license or copyright, see http://jap.aip.org/jap/copyright.jsp**